

## Research Papers

# Hourly analysis of temperature and heat gain reduction for building envelope-compacted phase change material in extremely hot conditions

Qudama Al-Yasiri<sup>a,b,c,\*</sup>, Márta Szabó<sup>b</sup>

<sup>a</sup> Doctoral School of Mechanical Engineering, MATE, Szent István campus, Páter K. u. 1, Gödöllő H-2100, Hungary

<sup>b</sup> Department of Building Engineering and Energetics, Institute of Technology, MATE, Szent István campus, Páter K. u. 1, Gödöllő H-2100, Hungary

<sup>c</sup> Department of Mechanical Engineering, Faculty of Engineering, University of Misan, Al Amarah City, Maysan Province 62001, Iraq



## ARTICLE INFO

## Keywords:

PCM  
Building energy  
Building envelope  
Surface temperature reduction  
Heat gain reduction

## ABSTRACT

Compacting phase change materials (PCMs) for thermal energy management in buildings is a promising method to reduce peak temperature and heat gain in hot climates. This experimental study analyses the hourly temperature reduction (HTR) and hourly heat gain reduction (HHGR) of building envelope-compacted PCM passively during a hot summer day. Two cubicles, one compact with PCM and the other without, are fabricated and examined under non-ventilated conditions concerning the supreme PCM thickness and position in the roof and the best thermally-performed PCM-bricks in the walls. The results showed that PCM effectiveness is time-dependent, and the east wall performed better than the other walls showing a maximum HTR of 9.1 % and HHGR of 16 %. Moreover, the PCM roof surface showed a maximum HTR and HHGR of 15.1 % and 34.9 %, respectively, contributing to the total HGR by one-third. The research exhibited that the PCM cubicle indoor temperature was reduced by up to 4 °C in comparison with the one referenced.

## 1. Introduction

Buildings are the primary consumer of national energy universally [1]. The International Energy Agency stated that the building envelope is responsible for 36 % of building energy consumption and around 39 % of CO<sub>2</sub> emissions [2]. Consequently, remarkable energy-saving potential could be accomplished by enhancing building envelope performance by applying different passive and active technologies. Recently, incorporating phase change materials (PCMs) with building construction has been introduced as a promising solution to increasing building dynamic thermal response and improving thermal comfort [3]. PCMs are unique materials that can absorb high heat within a limited volume compared with traditional construction materials [4]. Accordingly, the heat could be stored/charged throughout the day and dissipated/discharged at night, reducing the building's indoor temperature and shifting the peak load for better energy and comfort requirements [5,6].

Presently, several studies have been directed to explore the thermal improvement of building envelope elements and construction materials when PCMs applied, such as PCM roofs [7], PCM walls [8,9], PCM Trombe walls [10], PCM bricks [11], PCM wallboards [12], PCM windows [13], PCM floors [14], PCM ceiling [15], PCM insulation [16], PCM cementitious mortars [17] and plastering [18].

Shahcheraghian et al. [19] investigated the peak temperature and heat gains reduction of PCM macroencapsulated panels involved in one room's walls compared to another room without PCM (reference cubicle) under Tehran (Iran) weather conditions. Their experimental results showed that the average/peak temperature was reduced by 1.5 °C/2.3 °C in the PCM cubicle. Moreover, a maximum of 44 % heat gain reduction was achieved for the east wall of the PCM room compared to the reference one. Al-Rashed et al. [20] numerically deliberated the annual power consumption in arid buildings when PCM with 20 mm thickness and the suitable melting temperature were incorporated close to the interior edge. The locations were selected according to Köppen–Geiger classification [21], including Dubai City in Arab Emirates, Jeddah City in Saudi Arabia, Kuwait City in Kuwait and Lahore City in Pakistan. The results revealed that a power-saving of 55.47 %, 53.89 %, 58.86 % and 53.57 % can be achieved at these locations, respectively. The study designated that the finest PCM melting temperature for Lahore City and Dubai was in the range of 21 °C–23 °C and 23 °C–25 °C, respectively. At the same time, the PCM melting temperature range of 25 °C–27 °C was the best for Jeddah and Kuwait City locations. Tunçbilek et al. [22] explored the role of PCM loaded into bricks on building annual and seasonal thermal performance in the Marmara region, Turkey. They studied the ideal PCM transition

\* Corresponding author at: Doctoral School of Mechanical Engineering, MATE, Szent István campus, Páter K. u. 1, Gödöllő H-2100, Hungary.

E-mail addresses: [qudamaalyasiri@uomisan.edu.iq](mailto:qudamaalyasiri@uomisan.edu.iq) (Q. Al-Yasiri), [Szabo.marta@uni-mate.hu](mailto:Szabo.marta@uni-mate.hu) (M. Szabó).

<https://doi.org/10.1016/j.est.2023.107838>

Received 1 January 2023; Received in revised form 1 May 2023; Accepted 22 May 2023

Available online 1 June 2023

2352-152X/© 2023 The Author(s). Published by Elsevier Ltd. This is an open access article under the CC BY license (<http://creativecommons.org/licenses/by/4.0/>).

temperature among 18 °C–26 °C and found that the PCM temperature is varied depending on the season. On an annual basis, their analysis designated that the PCM of 18 °C transition temperature is optimum, decreasing the thermal energy by up to 17.6 %. Sun et al. [23] verified a parametric analysis to investigate the thermal enhancement of a wall loaded with passive PCM considering the outer and inner temperatures, layer thickness and position, and the optimal phase change temperature. Outcomes indicated heat flux decrease by up to 50 % at 7 mm PCM thickness and melting temperature between 27 °C and 31 °C with a fixed indoor air temperature of 24 °C. Saxena et al. [24] examined the temperature and heat transfer reduction when OM35 (35 °C) and Eicosane (36 °C–38 °C) macroencapsulated single/double containers involved inside bricks under climate conditions of Delhi (India). The results reported better thermal performance for Eicosane in which the brick's temperature and heat transfer was reduced by 4 °C–9.5 °C and 40 %–60 %, respectively, when single and double PCMs incorporated. In another Indian city, Sheeja et al. [25] investigated the annual room temperature reduction resulting from loading PCM of 29 °C melting point installed on the building's interior brick walls under Chennai city (India) climatic conditions. Numerical results presented that the room temperature was reduced by 6 °C in January and March, whereas a minimum reduction of 3 °C was achieved in May. For the building's indoor thermal management, Salgueiro et al. [26] fabricated and examined composite PCM comprised of a microencapsulated PCM (32 °C melting temperature), cement mortar and lightweight expanded clay granules. The results reported good thermal properties for the modified mortar with a thermal conductivity reduction of 24 % and a specific heat capacity increment of 17 % compared with the reference mortar without PCM. However, PCM addition increments shrinkage by 85 % and capillarity by 49 %, reducing by 20 % in the compressive and flexural strength. Wang et al. [27] numerically investigated the indoor thermal comfort and energy consumed by PCM wallboards installed in high-rise buildings under Shanghai conditions. The study revealed that the ideal transition temperature ranged between 20 °C and 26 °C, the thermal comfort range for occupants. Moreover, the PCM wallboards were more effective in the winter than in summer, and the best PCM transition temperature was season-reliant. In summer, the 24 °C melting temperature PCM wallboard installed on the east wall saved energy by 27.78 %, whereas the PCM of 22 °C installed on the south wall saved energy by 96.2 %. Al-Mudhafar et al. [28] analysed the peak-load shifting, peak temperature minimisation and temperature fluctuation reduction when RT-35 (29 °C–36 °C) was installed on a building roof, floor and walls under Baghdad and Basra, Iraq, climate conditions). The outcomes exhibited that the cooling load was abridged remarkably due to reduced heat gain, and the peak load was shifted by 5 h. Annual building energy and summer temperature reduction of PCMs incorporated in wooden buildings were studied by Wi et al. [29]. In their study, 22 types of shape-stabilised PCM (SSPCM) (paraffin and carbon-based materials), having phase change temperatures between 20 °C and 30 °C, were studied under weather conditions of Seoul (Korea). Numerical results showed that SSPCMs have averagely reduced annual energy consumption by 5 %, in which 479.8 kWh reduction was achieved at the best melting temperature ranging from 23 to 27 °C, and the summer peak temperature was minimised by 4.1 °C. Bohórquez-Órdenes et al. [30] numerically analysed the energy reduction and CO<sub>2</sub> emissions mitigation of R23C PCM (24 °C melting temperature) with 2–10 mm thickness incorporated building's external walls and ceiling under Santiago (Chile) climate conditions. Results showed that the thermal stress hours are minimised by 11 %–23 %, and the cooling load decreased by 45.4 %–60.3 % during summer. Furthermore, CO<sub>2</sub> emissions were mitigated by 60.3 % when 10 mm PCM was incorporated. Under Kuwait City climate, Al-Rashed et al. [31] numerically studied the heat gain and CO<sub>2</sub> emissions reduction when 20 mm PCM layer of RT-31 (27 °C–33 °C), RT-35 (29–36) and RT-42 (38–43) was installed on the interior of building roof and walls. They claimed that RT-31 PCM showed better effectiveness in which an annual energy and CO<sub>2</sub> emissions were saved by 481 kWh/m<sup>2</sup>

and 198.65 kgCO<sub>2</sub>/m<sup>2</sup>, respectively.

Sovetova et al. [32] explored the energy performance of thirteen different PCMs (20 °C to 30 °C transition temperature range) integrated building envelope under the desert climate of Mecca, Abu-Dhabi, Cairo, Dubai, Jodhpur, Nouakchott Faisalabad, and Biskra, considering the temperature fluctuations reduction, maximum temperature reduction and building energy-saving. Numerical findings indicated that higher PCM melting temperatures performed better, and the energy-saving varied from 17.97 % to 34.26 %. Hamidi et al. [33] quantified the benefits of combining PCMs (22 °C to 32 °C) into brick walls in different Mediterranean locations with the same approach. Numerical results revealed that up to 56 % of energy savings were achieved under north-east Mediterranean locations against no benefits for cities in the southeast. The study designated that PCM of 26 °C phase change temperature was appropriate in most locations. Rathore et al. [34] investigated the time delay, indoor peak temperature and thermal amplitude reduction when OM37 PCM (melting temperature of 39.1 °C) macroencapsulated pipes were buried inside the building envelope in Mathura (India). Experimental findings indicated average room temperature reduction by 0.2 °C to 4.3 °C, a maximum time delay of 97.5 min, and a decrement factor of 24.69 %.

According to the above literature, many numerical studies were verified to examine the PCM-compacted construction materials for reducing cooling load and saving energy compared to a minimal number of experiments. Most of these studies focused on monthly, seasonal and annual PCM thermal performance against limited ones that considered hour-by-hour PCM performance. Besides, experimental studies that consider all effective parameters of PCM integration, such as the best PCM thickness, effective position, best encapsulation area, etc., are limited, especially under severe hot locations. Therefore, this research aims to study the hourly temperature and heat gain reduction from compacting PCM passively into scaled rooms. The work is conducted for the thermally-worst building envelope combination under the hottest climate conditions in Iraq. The study conclusions are believed to deliver constructive information for specifying the effective hours for PCM and quantifying the highest benefits towards further modifications and optimization.

## 2. Experimental work

### 2.1. Description of cubicles

Two identical cubicles (1 × 1 × 1 m), one compacted with PCM and the other left with no PCM, were built and tested in the hot climate of Al Amarah, Maysan Province (Latitude: 31.84°E & Longitude: 47.14°N), Iraq. The cubicles are prepared using local materials for residential building constructions in the city. According to our previous local studies, these combinations are poor in thermal performance and result in high cooling loads [35]. The roofs were constructed from Isogam (a local roofing product used as a finishing layer), concrete (as roof layer) and gypsum mortar (as a cladding layer). Moreover, the brick walls were fabricated using concrete bricks (with 23 × 12 × 7 cm dimensions) and an outside cement mortar layer. Fig. 1 shows the main steps for preparing the concrete layer and bricks.

Cubicles were located on a building rooftop with an east direction to study the influence of solar radiation on all walls during the experiment day. Both cubicles are situated on dense woody foundations to guarantee no heat transfer from the floor. Each cubicle was provided with a small wooden-framed window (25 × 35 cm) mounted on the eastern wall of the cubicles. High-density foam was used to fill all slots and element connections to ensure no air leakage between the interior and exterior environments.

### 2.2. PCM panel/capsules

Petroleum paraffin wax was included in the PCM cubicle after careful

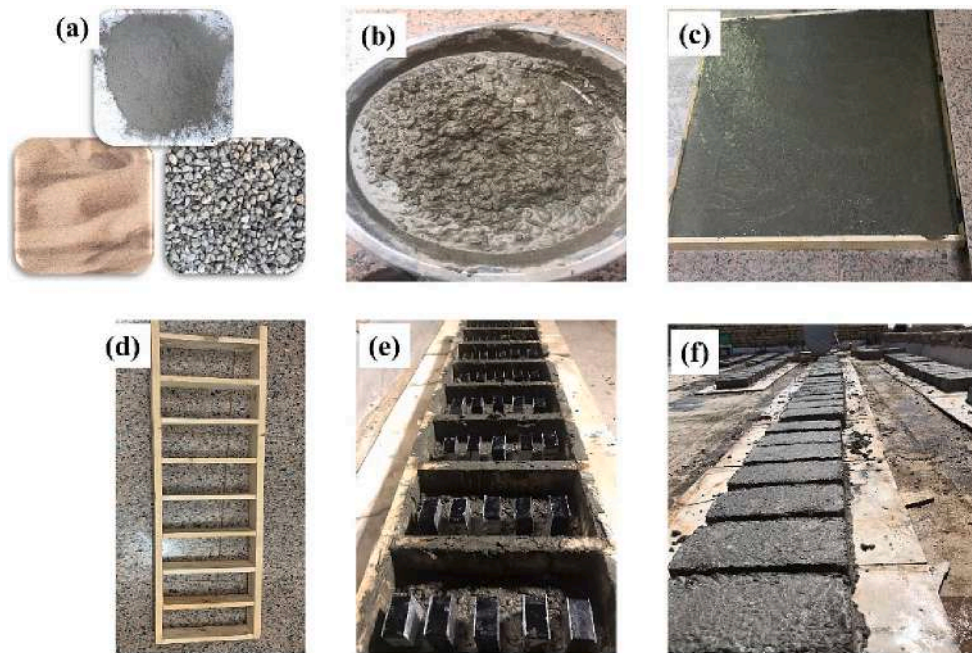


Fig. 1. Preparation of the concrete layers and bricks (a) raw materials (cement, sand and gravel), (b) concrete mixture, (c) concrete layer preparation, (d) mould of bricks, (e) preparation of PCM bricks, (f) solidified bricks.

macroencapsulation. This PCM has a melting temperature appropriate for the location under study, high latent fusion heat and relatively sharp melting/solidification temperature point, not to mention its local availability with low cost. Table 1 displays the features of the PCM.

The macroencapsulation technique was adopted in this work as it is the suitable method to preserve the PCM from leakage when incorporated with building materials and provide a suitable enhancement to the PCM thermal conductivity due to increased heat transfer area [37]. In this research, PCM macroencapsulated panel was involved within the roof, and aluminium containers/capsules were compacted in the bricks.

For the PCM cubicles' roof, a PCM panel made of galvanised steel (0.5 mm thickness sheet) was fabricated with 1 × 1 m to fit the roof area and a thickness of 1.5 cm. The panel was positioned between the PCM cubicles' finishing and main roof layers. Based on our previous studies, this thickness and position are the best-performed aspects [38,39]. A 7 kg PCM was included in the panel to guarantee excellent thermal behaviour with no leakage during phase transition. Conversely, the PCM compacted into concrete bricks was macroencapsulated inside square cross-sectional aluminium capsules. Compared with many other shapes and sizes, these containers/capsules had the best thermal performance when incorporated with concrete bricks [40]. Five PCM capsules (4 × 4 × 2 cm) with a PCM amount of 145 g were poured inside each PCM brick to construct the PCM cubicles' walls. These capsules were sealed well using high-quality thermal glue to prevent leakage and symmetrically distributed in the middle of each brick to retain their mechanical properties. Besides, the concrete bricks-comprised PCM capsules were flattened well to ensure the best capsules position with minimal air gaps, which minimises PCM leakage during the melting phase. Fig. 2 shows the preparation steps of the PCM panel and capsules.

Table 2 lists the detailed characteristics of the cubicle construction materials, and Fig. 3 shows the final experimental cubicles.

### 2.3. Thermal measurements and mechanical test

For thermal measurements, a data logger-based multi-channel Arduino (type Mega 2560) (manufactured and calibrated by Ardunic Co. [42]) was connected to thermocouples to measure envelope surface temperature and air temperatures. Ten T-type thermocouples from TEMPSENS of 0.2 mm direct contact bulb with a temperature working variety between -270 °C and 370 °C and precision of ±0.5 °C) were attached on the interior surface centre of roofs and walls for both reference and PCM cubicles. Besides, a sensor was positioned at the centre of cubicles to record the indoor air temperature, while another sensor was fixed outside the cubicles for outdoor temperature measurement. The Arduino was automated to measure temperatures each 30 min throughout the experiment and store them continuously in a portable microstorage memory connected to the Arduino. On the other hand, a handy solar power meter (Type SM206 with a range of 0.1–399.9 W/m<sup>2</sup> and accuracy of ±10 W/m<sup>2</sup>) was used to measure the incident solar radiation during the experiment daytime every 30 min. In addition, a thermal camera (model WB-80VOLT-CRAFT®) of a temperature sensor ranging from -20 °C to 600 °C and accuracy of ±2 % ±2 °C was used to show the temperature behaviour of outside surfaces temperature of cubicles at different times of the experiment. The LCD display of the thermal camera normally shows the photo in 4 colour palettes: IRON Red (red), colour RGB, grayscale (white heat), and grayscale (black heat), with no specific temperature range for each colour [43]. The thermocouple type used, solar power meter and

Table 1  
Characteristics of paraffin wax as tested by the producer [36].

PCM photo	Appearance	Melting point (°C)	Thermal conductivity (W/m.K)	Heat of fusion (kJ/kg)	Specific heat (kJ/kg.K)	Density (kg/m <sup>3</sup> )
	White	40–44	0.21	190	2.1	930 (solid) 830 (liquid)

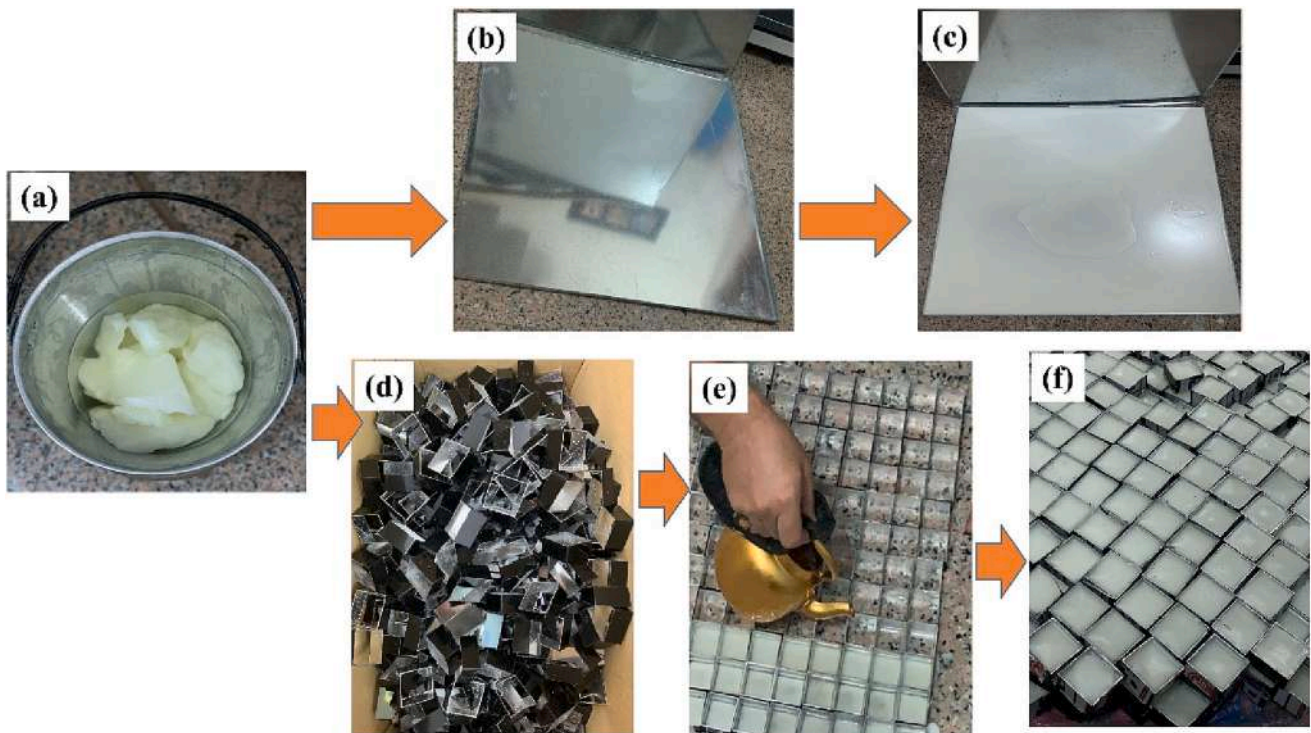


**Fig. 2.** Preparation of PCM panel/capsules (a) PCM melting process, (b) empty galvanised steel panel, (c) PCM-filled panel, (d) empty capsules, (e) PCM-filled capsules, (f) solidified PCM capsules (before capping).

**Table 2**

Characteristics of construction materials used to fabricate cubicles [41].

Material	Thickness (cm)	Thermal conductivity (W/m.K)	Density (kg/m <sup>3</sup> )
Isogam (roof)	0.4	0.35	1400
Concrete layer (1:2:4) (roof)	5	1.49	2300
Gypsum mortar (roof)	0.2	0.57	1200
Cement mortar (1:3) (walls)	1	0.99	2020
Concrete bricks (walls)	7	1.4	1440

thermal camera are shown in Fig. 4.

As indicated earlier, the PCM layer was integrated with the PCM cubicle's roof as a separate layer, while it was immersed as capsules into wall bricks, weakening their mechanical properties. Therefore, investigating the mechanical strength of PCM bricks is necessary to provide a clear vision of PCM compacting into the building structure. For this purpose, a crushing strength test was made for the PCM and bare bricks using a compression test machine (type ADR Touch head from ELE International) with a 2000 kN maximum load capacity. Six bricks were tested (three from each brick type), and the outcomes displayed that the maximum compression strength at the failure of bare bricks were 496.1, 481.5 and 503.2 kN, against 411, 315.2 and 338 kN for PCM bricks. These values are averagely equivalent to 17.88 and 12.84 N/mm<sup>2</sup> compression strength, considering the brick area of 27,600 mm<sup>2</sup>. Therefore, the compression strength of PCM bricks was reduced by ~28.2 % compared with the bare bricks. The decline of PCM brick strength is attributed to the poor mechanical strength of aluminium containers used for PCM encapsulation. Some photos of the mechanical test machine and PCM brick before and after the compression test are shown in Fig. 4.

### 3. Results and discussion

Buildings in Iraq are the primary energy consumers during the summer season due to the harsh weather conditions and the excessive use of air-conditioners to maintain adequate indoor thermal comfort. In this regard, residential buildings consume 48.3 % of the total energy provided by the national grid [44]. In Baghdad, the capital of Iraq, it was reported that houses consume about 69 % of electrical energy for cooling annually, and such a percentage could be decreased by up to 65.36 % by applying active or passive strategies on the building envelope [45]. The current research was conducted on a hot summer day, 15 September 2021, from 6:00 to 24:00 in the hot summer of Al Amarah, Maysan Province, in Iraq. September is among the hot summer months in the city, where the outdoor air temperature exceeds the limit of 45 °C on several days and the sunshine hours exceed 12 h, as indicated in Fig. 5-a. Besides, September days have a clear-sky with high solar insulation, especially at midday (Fig. 5-b).

#### 3.1. Exploration of surface temperature

Fig. 6 shows the temperature variation with 30 min time intervals of the indoor ( $T_i$ ) and inside surface temperatures ( $T_{in}$ ) for roofs and walls of experimental cubicles. In addition, the outdoor temperature ( $T_o$ ) and solar radiation (SR) are shown in each figure. As can be observed in all figures, the inside surface temperature of the reference cubicle elements was higher than that of the PCM cubicle during daytime hours. Nonetheless, the element inside surface temperature was opposed as soon as the daytime ended. This phenomenon occurs due to the PCM thermal behaviour that reduces the heat across the envelope elements in the daytime during the heat charging phase (melting phase). Besides, the charged heat (the heat accumulated inside the PCM) had released at night, increasing the elements' temperature of the PCM cubicle until they became at the same temperature level late at night. This temperature behaviour has resulted from the non-ventilated cubicles throughout the experiment, which keeps the outdoor temperature

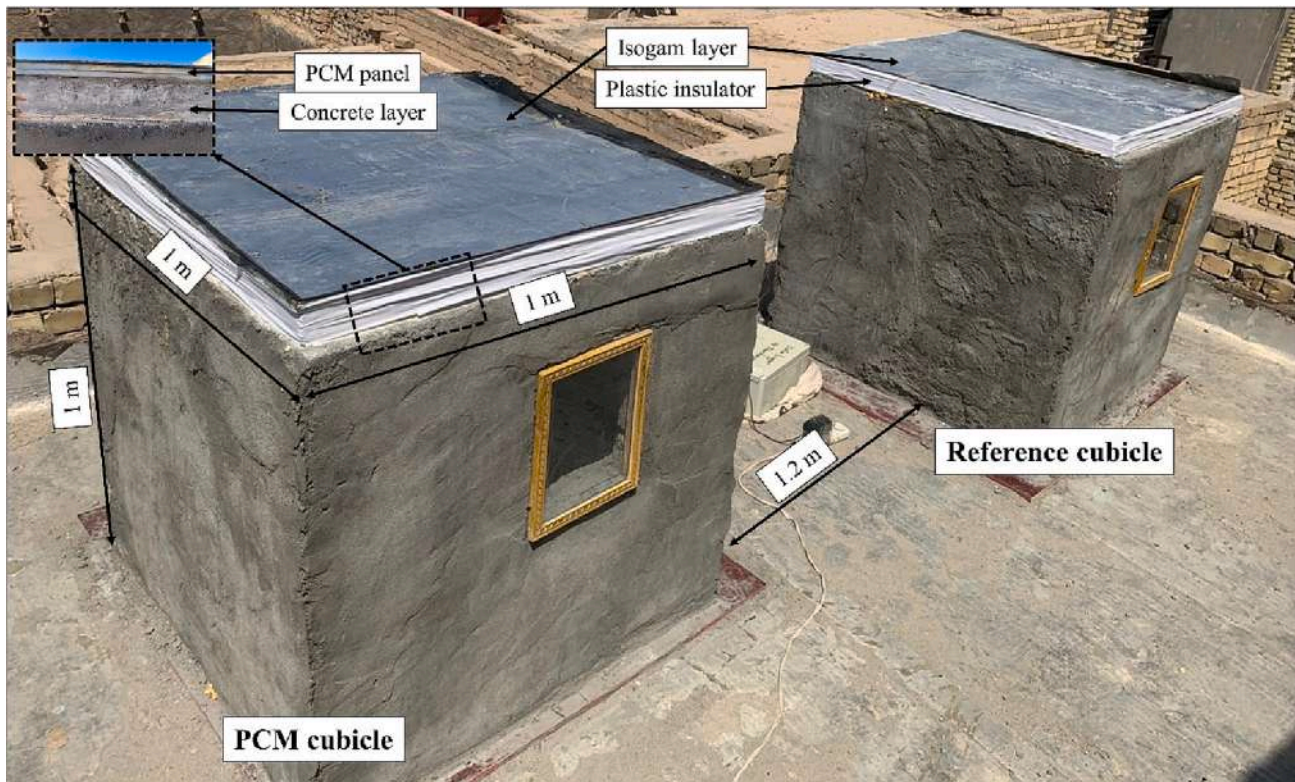


Fig. 3. 3D view of experimental cubicles.



Fig. 4. Photos of thermal measurement devices and mechanical test machine.

controlling the temperature variation during the thermal cycle. The figures also indicated that the highest inner surface temperatures lagged compared to the outside air temperature and sun radiation) as a result of the element's thermal resistance. However, the PCM cubicle's elements indicated noticeably extended time-shifting than the reference

cubicle elements. Fig. 6 shows that east-oriented walls exhibited the highest temperature gap of 2 °C–5.25 °C between 8:00 and 17:00, with the highest mark between 9:00 and 10:00. This temperature gap rapidly shrinks after 18:00, affected by the low ambient temperature at night. On the

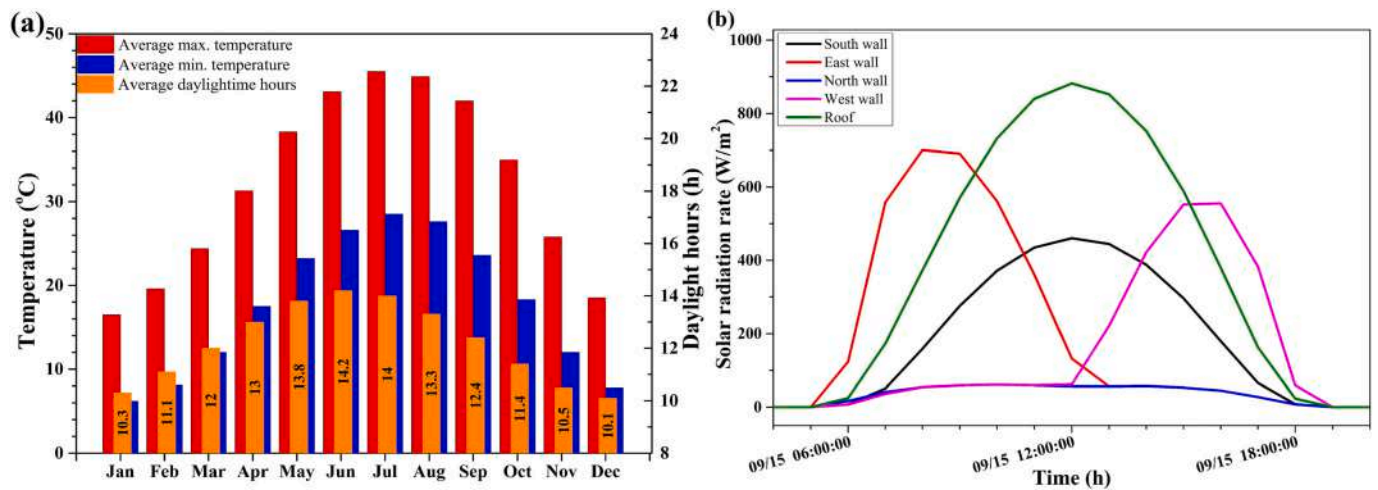


Fig. 5. Weather conditions [46] (a) average minimum/maximum temperature and daylight hours, (b) Solar radiation rate on roof and walls.

other hand, south-oriented walls showed a lower temperature gap of 1.25 °C–2.75 °C from 8:30 to 14:30, showing poorer PCM potential utilisation than the case of east-oriented walls. These walls have severely influenced the indoor environment temperature as they reached the mark of 57 °C around 17:00. The temperature behaviour of south-oriented walls was reversed earlier, even before the sunset at 18:00, till midnight. As indicated in Fig. 6, the west-oriented walls showed the poorest temperature behaviour regarding PCM utilisation, wherein the temperature gap was between 0.25 °C and 1.5 °C throughout the day. In contrast, north-oriented walls indicated a better temperature gap by an average of 2.25 °C from 8:30 to 14:30 (Fig. 6).

The temperature trend of roofs presented in Fig. 6 showed different temperature trends than walls. The temperature gap of roofs was large by up to 4.25 °C–6.5 °C between 9:00 and 15:00, showing a notable utilisation of PCM storage capacity. However, the PCM solidification phase (i.e., heat discharging) in the PCM cubicles' roof was not finished as in the walls and required more time to release the stored heat. This may be indorsed to that the roof stored massive heat in the PCM cubicle since it received high solar radiation all day long compared with the time-dependent walls. Besides, the PCM roof thermal mass was larger than the PCM walls due to the high compacted PCM amount that needed more time to be released completely.

The temperature variation of the indoor air of both cubicles (shown in Fig. 6) followed the same temperature variation trend as the roofs and walls, exceeding the comfort level range. The temperature gap was between 2.25 °C and 4.5 °C in the period 7:30–14:30 due to the accumulated heat of all elements. However, the temperature trend of indoor air was primarily similar to east walls and roofs during the daytime, indicating the considerable influence of these elements on indoor temperature throughout the peak time.

Fig. 7 shows numerous thermal camera images of the outside surface temperature of cubicles at different periods of the day. Starting from 6:00, the sun was partially incident on the north walls at a low rate, heating the outer surfaces equally by about 28 °C. At 9:00, the sun rises vertically, and most solar radiation incident on the east walls with a high ratio; thus, the outer surfaces are warming up with lots of heat passing towards the inside space. At this time, the PCM is in a charging phase, and heat is stored inside PCM capsules, making the middle of brick hotter than the outside and inside surfaces. This is observed clearly in the slight temperature difference of about 0.6 °C between the reference and PCM east walls at 9:00. Besides, the night coolness stored by PCM during the late night hours is released, making PCM elements colder than reference elements in the first few hours of the morning. The sun's position at noon is perpendicular to cubicles where the roofs and south walls receive high solar radiation. At this time, the PCM is expected to be

fully liquid inside capsules of the PCM cubicle south wall and heat charging is continuous. Therefore, some heat is dissipated uncontrollably towards inside and outside spaces due to the heat transfer difference between PCM capsules and indoor/outdoor environments. This behaviour is noticed in the relevant photos where the outer surface temperature variance concerning the PCM and reference south walls is 0.4 °C. At 15:00, the sun is perpendicular on the roofs and west walls, and the ambient temperature reaches high limits encountered with a high solar radiation rate. Therefore, the PCM liquid is at a high temperature, at this time, in the west wall and roof, resulting in high outside surface temperature compared with their corresponding elements in the reference cubicle. This is shown by the outside surface temperature difference of about 1.7 °C and 1.8 °C between the west walls and roofs, respectively. At 18:00, when the sun rises and ambient temperature drops, the discharging heat from PCM is expected to start due to the conductive and convective heat transfer difference between the PCM capsules and outdoor ambient temperature. As a result, the outside surfaces of the PCM cubicle dissipate heat at a larger rate than the reference cubicle outer surfaces. The temperature limit and heat dissipation time depend mostly on the ambient conditions (mainly the outdoor temperature and wind speed) and the amount of heat stored in the roof and walls. This can be detected clearly considering the inside surface temperature difference between PCM and reference roofs in Fig. 6 and their outside temperature difference of about 1.9 °C in Fig. 7.

### 3.2. Analysis of hourly temperature reduction

Reduced inside surface temperature is the main benefit of PCM when incorporated into building elements under hot locations, working as dynamic thermal insulation [47]. This reduction considerably influences thermal comfort and decreases the use of air-conditioning equipment and may avoid the need for such systems in transition seasons (i.e., spring and autumn).

In this research, a comparison between PCM and reference cubicles is studied during day time considering the inner surface temperature decrement and the impact on the indoor air temperature. Incidentally, the hourly temperature reduction (HTR) is calculated considering the hourly temperature difference (HTD) to explore the contribution of PCM. Accordingly, the TD was simply calculated as the inside surface temperature difference of every component in the PCM and reference cubicles each hour, based on Eq. (1) (indoor HTD was calculated considering the outside and indoor air temperature). Besides, the HTR was calculated as the ratio of HTD of each element in cubicles to the corresponding element surface temperature, according to Eq. (2), as follows:

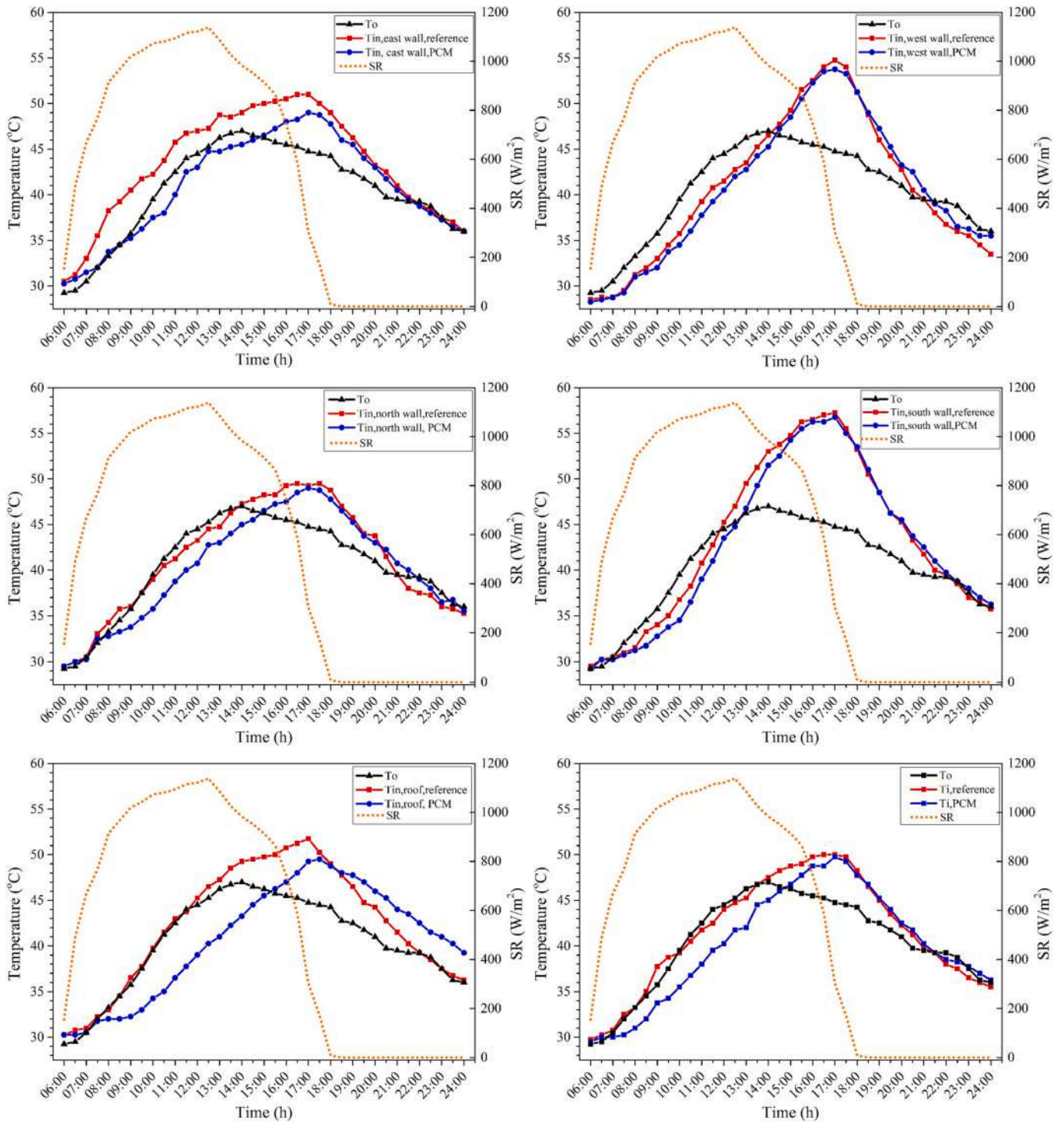


Fig. 6. Temperature variation of walls, roof and indoor air.

$$HTD = T_{s,ref} - T_{s,PCM} \tag{1}$$

$$HTR = \frac{HTD}{T_{s,ref}} \times 100\% \tag{2}$$

where  $T_{s,ref}$  and  $T_{s,PCM}$  are respectively the inside surface temperature (inside face) in the reference and PCM elements (°C).

Fig. 8 shows the HTD and HTR of each element. It is worth noting that the HTR was estimated during the day hours only since the PCM temperature behaviour is adverse during nighttime due to the heat dissipation of the PCM cubicle, as indicated earlier.

As shown in Fig. 8, all elements of the PCM cubicle recorded HTD and HTR by at least 0.25 °C and ~0.5 %, respectively. The east-oriented wall was designated the highest HTD and HTR compared with the other walls. The maximum HTD was attained at 11:00, reaching HTR by 9.1 % with HTD of 3.5 °C. The east walls directly received solar radiation at this time with an inclined sun position, resulting in the PCM melting phase earlier than other walls. On the other hand, the west-oriented wall exhibited the second-best thermal performance compared with the southern and northern walls. The highest HTR of the western wall reached at 13:00 with 8.5 % and HTD of 3.2 °C since the sun radiation

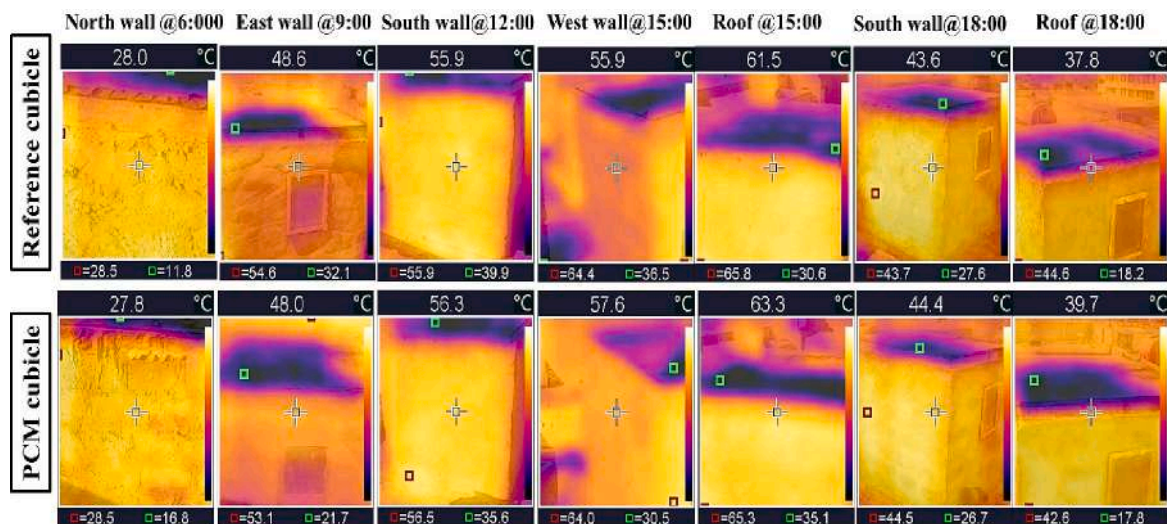


Fig. 7. Thermal images for outside cubicle elements at different times.

was hitting the west walls in the late afternoon. However, the PCM in the west wall was also effective before this time, influenced by the high ambient temperature from 9:00 to 13:00, as obviously shown in the HTR and HTD indicated in the relevant figure.

Surprisingly, the south-oriented wall indicated low HTR with a maximum of 5.6 % (HTD of 2.75 °C) at 13:00, although the sun was perpendicular in the midday period. The main cause is that the accumulated heat by the other elements in both cubicles during the first half of the day has influenced the south walls' inside surface temperature, making slight HTD between them. Fig. 6 supports this claim, showing that the surface temperature of the south walls exceeded 55 °C. Besides, the incident solar radiation hit the roofs when the sun was perpendicular at midday, with a minimal direct solar radiation rate on the south-oriented walls. Likewise, the north-oriented PCM wall showed poor thermal performance in terms of HTR, and this was expected since the solar radiation with a low rate was incident only in the early hours on the north walls. Therefore, the PCM involved in the north PCM wall did not reach its melting point, especially since the ambient air temperature was also low.

The PCM cubicle's roof showed the finest thermal performance compared with the walls during all daytime. The best performance was between 10:00 and 2:00, recording the highest HTD of 6.5 °C and HTR of about 15.1 % at 11:00. The considerable PCM roof performance compared with the walls is attributed to two main causes. Firstly, the high PCM quantity in the roof had charged more heat than walls. Secondly, the roofs were exposed to long-time direct solar radiation, which was advantageous for the PCM roof that exploited the PCM thermal storage potential compared with a negative impact on the reference roof.

The inside surface temperature improvement attained by PCM influences the inside temperature of the PCM cubicle, even though the experiment was conducted with no ventilation. In this regard, the heat accumulated continuously through the cubicle elements inside the PCM space and considerably lowered the indoor air temperature compared with the reference cubicle. This indicates PCM's benefits in reducing the peak load even during high outdoor temperatures and non-ventilated building envelope. The highest HTD and HTR in the indoor air were obtained at 9:00 with 4 °C and 10.6 %, respectively. Later, the HTR was decreased as the outdoor ambient temperature increased, and more heat crossed the cubicles' envelope towards the inside space. The reduction of such values significantly influences the indoor environment when considering the energy-saving for air-conditioning usage and thermal comfort attained. The HTD and HTR were adverse in the PCM cubicle at night due to the PCM solidification phase when stored diurnal heat was

released passively and uncontrollably as the outdoor ambient temperature decreased.

The results of HTD and HTR accomplished in this study are in good agreement (sometimes better) with the results of literature studies conducted in different hot locations. For instance, Rathore et al. [48] conducted an experimental study under Indian climate conditions (Mathura city) to determine the HTR for pipe-microencapsulated PCM buried into a concrete cubicle compared with another without PCM. Regardless of the low PCM melting temperature and the experimental site's outdoor ambient temperature compared with the current study, findings showed that all cubicle elements reported HTD and HTR ranging from 3.1 °C to 3.7 °C and from 7.19 % to 9.18 %, respectively. Under weather conditions of Chennai city, Beemkumar et al. [49] analysed the HTD of a concrete building roof integrated with PCM macro-encapsulated inside rectangular-shaped aluminium containers. The results showed an average HTD of 1 °C–2 °C compared with the standard concrete roof. Sovetova et al. [50] analysed thirteen PCMs with phase change temperatures varying between 20 °C and 32 °C, applied as a separate PCM panel of 20 mm thickness in the roof and walls of a typical building located in the United Arab Emirates. Simulation findings showed that the indoor air temperature was decreased by 1.09 °C at the optimum PCM melting temperature of 32 °C. Ramakrishnan et al. [51] conducted research on shape-stabilised PCM (SSPCM) consisting of paraffin (RT27) combined with hydrophobic expanded perlite (PCM carrier) to be used as plastering mortar for cladding interior walls and floor under Melbourne (Australia) climate conditions. The main findings reported HTD in the inner surface by 3.7 °C and indoor air decrease by 2.4 °C. Following the same incorporation method, Wi et al. [52] have also investigated SSPCM fabricated from *n*-Octadecane/expanded vermiculite and expanded perlite in a panel form applied for the interior envelope. The experimental results were performed using a climate chamber and revealed that the HTD of the SSPCM panel surface was decreased by 1.6 °C against the standard panel without SSPCM.

### 3.3. Analysis of hourly heat gain reduction

The heat gain (HG) concept describes how much heat is generated inside the building space due to inside and outside cooling load sources [53]. The HG could be exterior when it comes through the envelope elements from outside due to temperature difference (also called solar gain, the core of this research) or interior HG generated from the appliances inside the building space [54]. Quantifying the building envelope HG is necessary for measuring the cooling requirements inside buildings by considering the building envelope elements' thermal

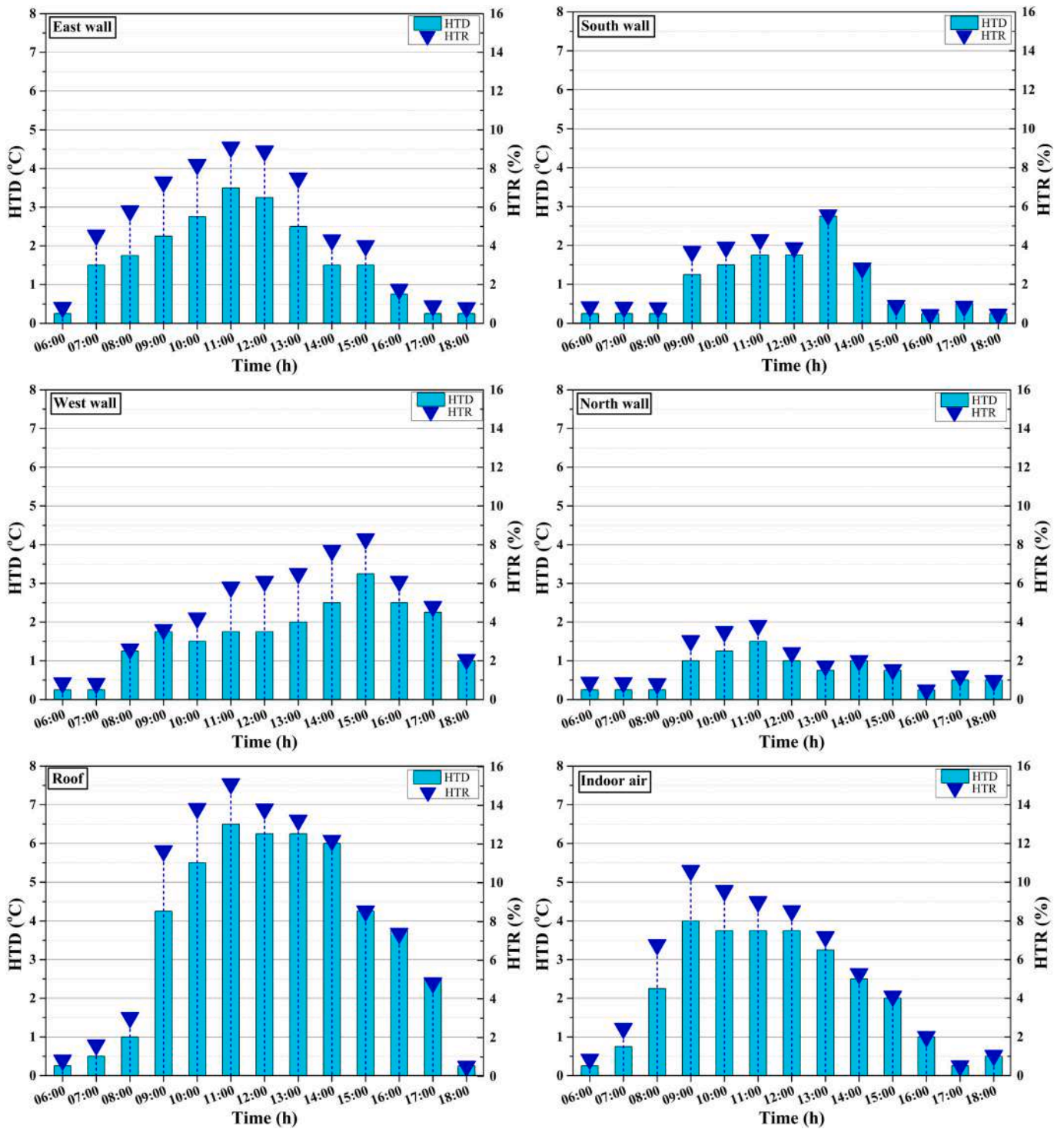


Fig. 8. HTD and HTR during daytime hours.

resistance against the heat flow from outdoor conditions [55]. In this research, the HG was estimated by Eq. (3) [56] as follows:

$$HG = h_{in} A (T_s - T_{in}) \quad (3)$$

where  $h_{in}$  is the convective-radiative heat transfer coefficient for interior elements (the value  $8.29 \text{ W/m}^2 \cdot \text{°C}$  was used for walls, and  $6.13 \text{ W/m}^2 \cdot \text{°C}$  was considered for the roof calculations [57]).  $A$  is the inside element area ( $\text{m}^2$ ),  $T_s$  is the element inside surface temperature, and  $T_{in}$  is the indoor temperature.  $T_{in}$  refers to the indoor design temperature, not the dry bulb temperature measured in the experiment. Therefore,  $T_{in}$

was kept constant ( $=24 \text{ °C}$ ) in the calculations to explore the heat gain of elements.

Accordingly, the hourly heat gain reduction (HHGR) attained in the PCM cubicle against the reference cubicle was quantified taking into consideration the HG of each corresponding element of experimental cubicles (%), according to Eq. (4) as follows:

$$HHGR = \left( 1 - \frac{HG_{PCM}}{HG_{ref.}} \right) \times 100\% \quad (4)$$

where  $HG_{ref.}$  and  $HG_{PCM}$  are respectively the heat gain each hour of

experimental cubicle elements (W).

The calculated results of the HHGR of the PCM elements against the reference elements during daytime are shown in Fig. 9. The HHGR during the nighttime was not considered due to the reversed behaviour of PCM cubicle elements during the solidification phase due to non-ventilation, as highlighted previously.

As a general finding in Fig. 9, the roof showed HHGR higher than all elements, whereas the east-oriented wall displayed greater HHGR than walls. The HHGR of the eastern wall was high between 9:00 and 13:00 since the east walls were visible to the beam solar radiation through this period. The PCM wall was interrupting and storing the heat coming from outdoor while passing quickly through the reference wall. The highest HHGR was achieved at 11:00 and 12:00 by about 16 % and 14.1 %, respectively. Later, the HHGR dropped for the rest of the day when PCM reached a full melting state and could not store more heat.

Similarly, the west-oriented PCM wall showed high HHGR reaching the highest reduction of about 12.9 % at 15:00 since the west-oriented walls remained directed to the sun radiation until late afternoon. This behaviour is apparently due to increased outdoor air temperature during midday that influences the PCM inside the west-oriented PCM wall. Nevertheless, the PCM was expected to reach its melting temperature at midday, and the PCM was in the melting phase along late afternoon. It is worth mentioning that the accumulated heat inside cubicles resulting from the other walls and windows in the first-half of the daytime affected the elements' inside surface temperature in the second-half, including the west walls.

The south-oriented PCM wall exhibited relatively poorer HHGR than the east-oriented wall. However, it experienced a long-time high ambient temperature as the east PCM wall. This may be elucidated that the south PCM wall did not collect beam solar radiation as much as the east PCM wall (as indicated in Fig. 5-b), which influenced the PCM effectiveness. However, the south PCM wall reached the highest HHGR of 13.3 % at 13:00 and drastically decreased afterwards. This is shown in Fig. 6 and Fig. 7, wherein the south-oriented walls reached the maximum inner surface temperature difference. From the other side, the north-oriented walls showed the poorest HHGR compared with other walls, as expected, since these walls were exposed to slight radiation only during the first morning hours. The highest HHGR attained by the north PCM wall was 10 % at 9:00, influenced by the increased ambient

temperature. Referring to the HHGR trend of the north PCM wall in Fig. 9, it can be stated that the PCM was ineffective at this wall and should be considered when conducting optimisation studies.

The roof, as expected, showed the highest HHGR, reaching a maximum of 34.9 % at 10:00, making this element the main contributor to the total HHGR by about one-third. However, the east-oriented PCM wall showed higher HHGR from 7:00 to 8:00 than the PCM roof due to the sun's position concerning these elements. Besides, the solar absorptivity difference of Isogam (in the roof) compared with the cement plaster of the wall has speeded the heat transfer in the latter element, which activated the PCM earlier. The continuously increased HHGR of the roof compared with the walls might be attributed to the great PCM quantity compacted and the roof thermal resistance compared with the thin layers of walls. These reasons expand the PCM melting inside the panel (compared with the capsules), which offers more insulation for the PCM roof. However, the positive behaviour of the PCM roof had negatively influenced the HHGR during the night period, which was the poorest compared with walls due to the considerable amount of stored heat. This keeps the PCM roof's inner surface temperature high until the end of the thermal cycle, as indicated in Fig. 6.

Total HHGR can be quantified by summing the HHGR of all elements following the same concept of [48] to calculate the total cooling load reduction through building elements. Accordingly, the PCM-incorporated cubicle resulted in an average HHGR of 48.7 % during day hours compared with the reference cubicle. These findings are remarkable compared with the studies conducted in different locations worldwide. For instance, Lei et al. [58] reported that the HG reduction (HGR) could attain the mark of 40.7 % under tropical Singapore weather conditions when PCM with 28 °C phase change temperature of 10 mm layer was applied to the exterior building walls surface. Rai [59] investigated the HGR when PCM incorporated different brick masonry wall configurations under Indian summer conditions and found that peak HGR of 9.9 % to 45.2 % could be achieved considering the wall orientation, outdoor ambient temperature and night ventilation effect. Kishore et al. [60] verified a numerical study on the PCM-integrated walls in various locations in the United States, considering different PCM melting temperatures, layer thicknesses and positions within the walls and reported an annual HGR of 3.5 %–47.2 % could be achieved. In the Middle Eastern countries, Amirahmad et al. [61] numerically

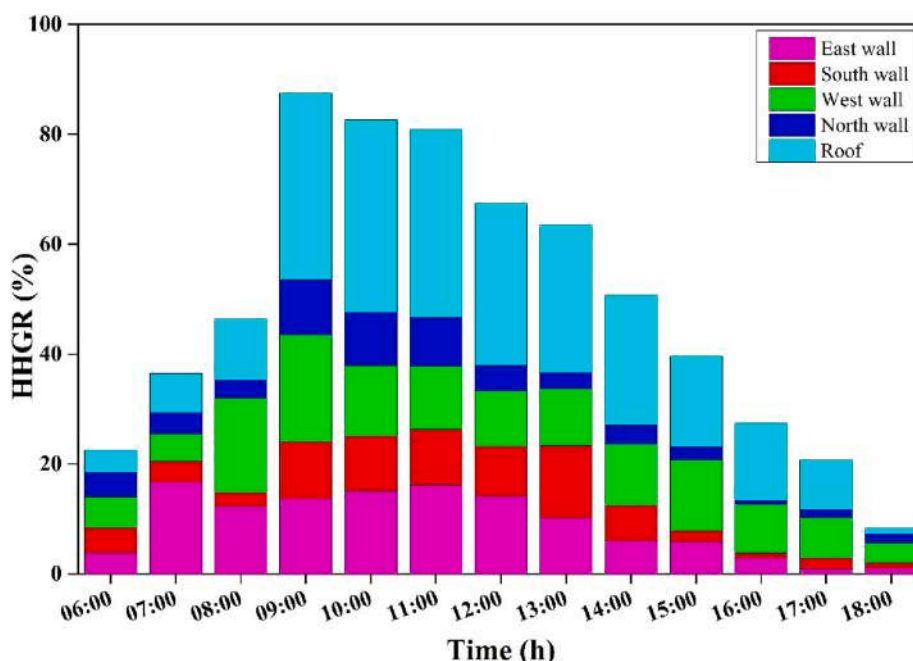


Fig. 9. HHGR during daytime.

analysed PCM loading (RT-27) into the building walls in parallel with an absorption chiller driven by a solar system concerning the hot and arid conditions for Najran City, Saudi Arabia. They reported HGR by up to 21 % during July. In comparison, Alqallaf and Alawadhi [62] conducted a numerical and experimental study under Kuwait City weather conditions for PCM integration with cylindrical holes in the roof. They reported HGR by 9 %–17.26 % subjected to the PCM type, functioning hours and operation month.

By the end of this analysis, it is worth highlighting that the results presented in this paper were superior to the findings reported in the literature studies as indicated above and give a pure indication of the building HHGR considering all elements. Moreover, these experimental findings provide a clear understanding of the HHGR of buildings under severe hot climates, allowing for further optimisation in the PCM application under these limitedly investigated locations. Besides, the findings of the current study are mostly in line with many literature studies conducted experimentally and numerically under various weather conditions worldwide. Table 3 briefly highlights the main results of recent studies focusing on temperature and heat gain advancements against the findings of current work.

#### 4. Conclusion

This research experimentally studied the hourly temperature and heat gain reduction in the building envelope elements when compacted with PCM during a hot summer day in Iraq. Two identical cubicles were built in which the PCM was compacted passively into the envelope elements of one of them, and the other was left without PCM for comparison. The thermal performance and temperature behaviour of both cubicles were studied for a non-conditioned case to examine the temperature behaviour during heat charging and discharging and the influence of outdoor ambient temperature. In general, the PCM compacted cubicle considerably enhanced the cubicle's thermal performance by reducing the hourly inner surface temperature and heat gain during the daytime. Moreover, several conclusions are drawn from the results obtained, as follows:

- The PCM cubicle indoor temperature was decreased by as much as 10.6 % (equivalent to about 4 °C temperature difference) during the day compared with the reference cubicle, showing a considerable enhancement in the built environment due to PCM compacting even

when applied under high diurnal temperatures and non-ventilated space.

- The highest PCM effectiveness is time-dependent regarding the sun's position during the day. The east-oriented wall and roof performed better during the first daytime hours, whereas the west-oriented wall achieved superior performance in the late afternoon.
- Among walls, the east-oriented PCM wall showed the greatest hourly temperature and heat gain reduction on average, reaching a maximum inside surface temperature and heat gain reduction of 9.1 % and 16 %, respectively. The west wall showed the best-second average inside surface temperature reduction.
- The PCM roof indicated the highest hourly temperature and heat gain reduction than walls, with 15.1 % and 34.9 %, respectively. Therefore, the roof was responsible for about one-third of the PCM cubicle's temperature and heat gain reduction. However, the roof showed poor thermal performance during solidification due to the high stored heat during daytime hours.
- The inside temperature of elements surfaces and indoor air were influenced after midday due to accumulated heat inside the cubicles with no ventilation. Therefore, proper ventilation should be considered at night to maintain the negative PCM thermal behaviour.
- Photos of the thermal camera showed that the PCM cubicle's outside surface temperature is higher than that of the reference cubicle after midday due to the remarkable heat difference between the melted PCM and outdoor ambient temperature. The outer surface of the PCM roof dissipated heat at higher temperatures and longer time than PCM walls due to the high amount of stored heat during day hours.

The experimental outcomes of this study are restricted to the construction materials, PCM type, cubicle size and location investigated in this work. Therefore, some other aspects will be studied in future to continue this work, including the effect of enlarged cubicle/room size, night ventilation (in terms of window orientation and window-to-wall ratio) and other passive techniques.

#### CRediT authorship contribution statement

**Qudama Al-Yasiri:** Conceptualization, Methodology, Data curation, Formal analysis, Investigation, Writing – original draft, Writing – review & editing. **Márta Szabó:** Conceptualization, Formal analysis, Investigation, Writing – review & editing, Supervision, Funding acquisition.

**Table 3**  
Summary of literature and current study findings.

Authors	Study location	Study type	PCM melting point (°C)	PCM integration method	Main findings of the study
Hamdani et al. [63]	Ghardaïa, Algeria	Numerical	20–26	Wallboard	<ul style="list-style-type: none"> <li>• Annual indoor temperature minimised by 2.36 °C–4 °C.</li> </ul>
Rangel et al. [64]	Monterrey city, Mexico	Experimental	29	Sheets	<ul style="list-style-type: none"> <li>• Average indoor temperature reduction by 4 %–7 %</li> </ul>
Saikia et al. [65]	Delhi, India	Experimental + numerical	29.85 and 35.85	Separate layer	<ul style="list-style-type: none"> <li>• Total HG reduction by 33.5 %.</li> </ul>
Sharma and Rai [66]	Delhi, India	Numerical	24–50	Separate layer	<ul style="list-style-type: none"> <li>• Summer HG reduction by 10.4 %–26.6 % and 12.6 %–36.2 % for PCM-enhanced walls and roof, respectively.</li> <li>• Average indoor temperature reduction by 3 °C.</li> </ul>
Elawady et al. [67]	Aswan City, Egypt	Numerical	27, 33, 36 and 48	Separate layer	<ul style="list-style-type: none"> <li>• Annual average wall surface temperature reduction by 1.5 %.</li> <li>• Indoor temperature reduction by 20.8 %.</li> </ul>
Elmarghany et al. [68]	Egypt	Experimental + numerical	33, 38, 43 and 48	PCM-filled brick wall	<ul style="list-style-type: none"> <li>• Annual average wall surface temperature reduction by 1.5 %.</li> <li>• Indoor temperature reduction by 20.8 %.</li> </ul>
Cárdenas-Ramírez et al. [69]	Lab work	Experimental	19.62, 31.51, and 53.85	Shape-stabilised PCM-based plaster	<ul style="list-style-type: none"> <li>• HG reduction by 1.5 %.</li> </ul>
Sangwan et al. [70]	Darwin, Australia	Numerical	24	Gypsum wallboard	<ul style="list-style-type: none"> <li>• HG reduction by 1.5 %.</li> </ul>
Kumar et al. [72]	Chennai City, India	Experimental	26–29	Hollow-brick composite	<ul style="list-style-type: none"> <li>• Monthly indoor temperature reduction by 2 °C–6 °C.</li> </ul>
Current study	Al Amarah City, Iraq	Experimental	40–44	Separate PCM panel in the roof + immersed capsules in bricks	<ul style="list-style-type: none"> <li>• Maximum indoor temperature minimised by 4 °C.</li> <li>• Maximum HG reduction by 16 % in the east-oriented wall and 34.9 % in the roof.</li> </ul>

## Declaration of competing interest

The authors declare that they have no known competing financial interests or personal relationships that could have appeared to influence the work reported in this paper.

## Data availability

Data will be made available on request.

## Acknowledgements

The first author would like to appreciate the administrative and financial support of the Stipendium Hungaricum Scholarship Program and the Doctoral School of Mechanical Engineering, MATE-Szent István campus, Gödöllő, Hungary, during PhD studies.

## References

- [1] IEA (International Energy Agency), The future of cooling: opportunities for energy-efficient air conditioning. <https://pronto-core-cdn.prontomarketing.com/449/wp-content/uploads/sites/2/2018/06/Melanie-Slade-The-Future-of-Cooling-Opportunities-for-Energy-Efficient-Air-Conditioning.pdf>, 2018.
- [2] IEA (International Energy Agency), UN Environment Programme, 2019 global status report for buildings and construction: towards a zero-emission, efficient and resilient buildings and construction sector. <https://www.worldgbc.org/news-media/2019-global-status-report-buildings-and-construction>, 2019.
- [3] J. Hu, X. Yu, Thermo and light-responsive building envelope: energy analysis under different climate conditions, *Sol. Energy* 193 (2019) 866–877, <https://doi.org/10.1016/j.solener.2019.10.021>.
- [4] J. Košny, PCM-Enhanced Building Components: An Application of Phase Change Materials in Building Envelopes and Internal Structures, Springer, 2015, <https://doi.org/10.1007/978-3-319-14286-9>.
- [5] J.R. Patel, V. Joshi, M.K. Rathod, Thermal performance investigations of the melting and solidification in differently shaped macro-capsules saturated with phase change material, *J. Energy Storage* 31 (2020), 101635, <https://doi.org/10.1016/j.est.2020.101635>.
- [6] M. Jurčević, S. Nizetić, M. Arıcı, P. Ocloń, Comprehensive analysis of preparation strategies for phase change nanocomposites and nanofluids with brief overview of safety equipment, *J. Clean. Prod.* 274 (2020), 122963, <https://doi.org/10.1016/j.jclepro.2020.122963>.
- [7] J. Hu, X. (Bill) Yu, Adaptive building roof by coupling thermochromic material and phase change material: energy performance under different climate conditions, *Constr. Build. Mater.* 262 (2020), 120481, <https://doi.org/10.1016/j.conbuildmat.2020.120481>.
- [8] E. Tunçbilek, M. Arıcı, M. Krajčák, S. Nizetić, H. Karabay, Thermal performance based optimization of an office wall containing PCM under intermittent cooling operation, *Appl. Therm. Eng.* 179 (2020), 115750, <https://doi.org/10.1016/j.applthermaleng.2020.115750>.
- [9] M. Arıcı, F. Bilgin, M. Krajčák, S. Nizetić, H. Karabay, Energy saving and CO<sub>2</sub> reduction potential of external building walls containing two layers of phase change material, *Energy* 252 (2022), 124010, <https://doi.org/10.1016/j.energy.2022.124010>.
- [10] X. Liu, Y. Zhou, G. Zhang, Numerical study on cooling performance of a ventilated Trombe wall with phase change materials, *Build. Simul.* 11 (2018) 677–694, <https://doi.org/10.1007/s12273-018-0434-z>.
- [11] Y. Gao, F. He, X. Meng, Z. Wang, M. Zhang, H. Yu, W. Gao, Thermal behavior analysis of hollow bricks filled with phase-change material (PCM), *J. Build. Eng.* 31 (2020), 101447, <https://doi.org/10.1016/j.job.2020.101447>.
- [12] C. Li, H. Yu, Y. Song, Y. Tang, P. Chen, H. Hu, M. Wang, Z. Liu, Experimental thermal performance of wallboard with hybrid microencapsulated phase change materials for building application, *J. Build. Eng.* 28 (2020), 101051, <https://doi.org/10.1016/j.job.2019.101051>.
- [13] D. Li, B. Wang, Q. Li, C. Liu, M. Arıcı, Y. Wu, A numerical model to investigate non-gray photothermal characteristics of paraffin-containing glazed windows, *Sol. Energy* 194 (2019) 225–238.
- [14] P. Devaux, M.M. Farid, Benefits of PCM underfloor heating with PCM wallboards for space heating in winter, *Appl. Energy* 191 (2017) 593–602, <https://doi.org/10.1016/j.apenergy.2017.01.060>.
- [15] Y. Khattari, A. Arid, A. El Ouali, T. Kousksou, I. Janajreh, E. Mahjoub Ben Ghoulam, CFD study on the validity of using PCM in a controlled cooling ceiling integrated in a ventilated room, *Dev. Built Environ.* 9 (2022) 100066, <https://doi.org/10.1016/j.dibe.2021.100066>.
- [16] C. Jia, X. Geng, F. Liu, Y. Gao, Thermal behavior improvement of hollow sintered bricks integrated with both thermal insulation material (TIM) and Phase-Change Material (PCM), *Case Stud. Therm. Eng.* 25 (2021), 100938, <https://doi.org/10.1016/j.csite.2021.100938>.
- [17] F. Orsini, P. Marrone, S. Santini, L. Sguerri, F. Asdrubali, G. Baldinelli, F. Bianchi, A. Presciutti, Smart materials: cementitious mortars and PCM mechanical and thermal characterization, *Materials (Basel)* 14 (2021) 4163, <https://doi.org/10.3390/ma14154163>.
- [18] Y. Kusama, Y. Ishidoya, Thermal effects of a novel phase change material (PCM) plaster under different insulation and heating scenarios, *Energy Build.* 141 (2017) 226–237, <https://doi.org/10.1016/j.enbuild.2017.02.033>.
- [19] A. Shahcheraghian, R. Ahmadi, A. Malekpour, Utilising latent thermal energy storage in building envelopes to minimise thermal loads and enhance comfort, *J. Energy Storage* 33 (2020), 102119, <https://doi.org/10.1016/j.est.2020.102119>.
- [20] A.A.A.A. Al-Rashed, A.A. Alnaqi, J. Alsarraf, Usefulness of loading PCM into envelopes in arid climate based on Köppen–Geiger classification - annual assessment of energy saving and GHG emission reduction, *J. Energy Storage* 43 (2021), 103152, <https://doi.org/10.1016/j.est.2021.103152>.
- [21] Köppen–Geiger Classification. <https://www.britannica.com/science/Koppen-climate-classification>, 2023.
- [22] E. Tunçbilek, M. Arıcı, S. Bouadila, S. Wonorahardjo, Seasonal and annual performance analysis of PCM-integrated building brick under the climatic conditions of Marmara region, *J. Therm. Anal. Calorim.* 141 (2020) 613–624, <https://doi.org/10.1007/s10973-020-09320-8>.
- [23] X. Sun, Y. Zhang, K. Xie, M.A. Medina, A parametric study on the thermal response of a building wall with a phase change material (PCM) layer for passive space cooling, *J. Energy Storage* (2021), 103548, <https://doi.org/10.1016/j.est.2021.103548>.
- [24] R. Saxena, D. Rakshit, S.C. Kaushik, Experimental assessment of phase change material (PCM) embedded bricks for passive conditioning in buildings, *Renew. Energy* 149 (2020) 587–599, <https://doi.org/10.1016/j.renene.2019.12.081>.
- [25] R. Sheeja, S. Kumar, P. Chandrasekar, A.J.S. Jospher, S. Krishnan, Numerical analysis of energy savings due to the use of PCM integrated in lightweight building walls, *IOP Conf. Ser. Mater. Sci. Eng.* 923 (2020) 12070, <https://doi.org/10.1088/1757-899X/923/1/012070>.
- [26] T. Salgueiro, A. Samagaio, M. Gonçalves, A. Figueiredo, J. Labrincha, L. Silva, Incorporation of phase change materials in an expanded clay containing mortar for indoor thermal regulation of buildings, *J. Energy Storage* 36 (2021), 102385, <https://doi.org/10.1016/j.est.2021.102385>.
- [27] H. Wang, W. Lu, Z. Wu, G. Zhang, Parametric analysis of applying PCM wallboards for energy saving in high-rise lightweight buildings in Shanghai, *Renew. Energy* 145 (2020) 52–64, <https://doi.org/10.1016/j.renene.2019.05.124>.
- [28] A.H.N. Al-Mudhafar, M.T. Hamzah, A.L. Tarish, Potential of integrating PCMs in residential building envelope to reduce cooling energy consumption, *Case Stud. Therm. Eng.* 27 (2021), 101360, <https://doi.org/10.1016/j.csite.2021.101360>.
- [29] S. Wi, S.J. Chang, S. Kim, Improvement of thermal inertia effect in buildings using shape stabilized PCM wallboard based on the enthalpy-temperature function, *Sustain. Cities Soc.* 56 (2020), 102067, <https://doi.org/10.1016/j.scs.2020.102067>.
- [30] J. Bohórquez-Órdenes, A. Tapia-Calderón, D.A. Vasco, O. Estuardo-Flores, A. N. Haddad, Methodology to reduce cooling energy consumption by incorporating PCM envelopes: a case study of a dwelling in Chile, *Build. Environ.* 206 (2021), 108373, <https://doi.org/10.1016/j.buildenv.2021.108373>.
- [31] A.A.A.A. Al-Rashed, A.A. Alnaqi, J. Alsarraf, Energy-saving of building envelope using passive PCM technique: a case study of Kuwait City climate conditions, *Sustain. Energy Technol. Assess.* 46 (2021), 101254, <https://doi.org/10.1016/j.seta.2021.101254>.
- [32] M. Sovetova, S.A. Memon, J. Kim, Thermal performance and energy efficiency of building integrated with PCMs in hot desert climate region, *Sol. Energy* 189 (2019) 357–371, <https://doi.org/10.1016/j.solener.2019.07.067>.
- [33] Y. Hamidi, Z. Aketouane, M. Malha, D. Bruneau, A. Bah, R. Goiffon, Integrating PCM into hollow brick walls: toward energy conservation in Mediterranean regions, *Energy Build.* 248 (2021), 111214, <https://doi.org/10.1016/j.enbuild.2021.111214>.
- [34] P.K.S. Rathore, S.K. Shukla, N.K. Gupta, Yearly analysis of peak temperature, thermal amplitude, time lag and decrement factor of a building envelope in tropical climate, *J. Build. Eng.* 31 (2020), 101459, <https://doi.org/10.1016/j.job.2020.101459>.
- [35] Q. Al-Yasiri, M.A. Al-Furaiji, A.K. Alshara, Comparative study of building envelope cooling loads in Al-Amarah city, Iraq, *J. Eng. Technol. Sci.* 51 (2019) 632–648, <https://doi.org/10.5614/j.eng.technol.sci.2019.51.5.3>.
- [36] Ministry of Oil, Midland Refineries Company. <https://mrc.oil.gov.iq/?dispatch>, 2022.
- [37] Q. Al-Yasiri, M. Szabó, Effect of encapsulation area on the thermal performance of PCM incorporated concrete bricks: a case study under Iraq summer conditions, *Case Stud. Constr. Mater.* 15 (2021), e00686, <https://doi.org/10.1016/j.cscm.2021.e00686>.
- [38] Q. Al-Yasiri, M. Szabó, Case study on the optimal thickness of phase change material incorporated composite roof under hot climate conditions, *Case Stud. Constr. Mater.* 14 (2021), e00522, <https://doi.org/10.1016/j.cscm.2021.e00522>.
- [39] Q. Al-Yasiri, M. Szabó, Experimental evaluation of the optimal position of a macroencapsulated phase change material incorporated composite roof under hot climate conditions, *Sustain. Energy Technol. Assess.* 45 (2021), 101121, <https://doi.org/10.1016/j.seta.2021.101121>.
- [40] Q. Al-Yasiri, M. Szabó, Thermal performance of concrete bricks based phase change material encapsulated by various aluminium containers: an experimental study under Iraqi hot climate conditions, *J. Energy Storage* 40 (2021), 102710, <https://doi.org/10.1016/j.est.2021.102710>.
- [41] Ministry of Construction and Housing-Ministry of Planning, Thermal Insulation Blog (Iraqi Construction Blog), 2013. <https://amanatbaghdad.gov.iq/amanarules/pict/جدونالحراريالزل/blog2013.pdf>.
- [42] Arduinic, Arduinic Sinaa, Baghdad, Iraq. <https://ardunic.com/auth>, 2020.

- [43] Conrad Electronic International GmbH & CoKG, VOLTcraft WB-80 IR camera -20 up to 600 °C 32 x 32 Pixel 9 Hz Built-in digital camera. <https://www.conrad.com/p/voltcraft-wb-80-ir-camera-20-up-to-600-c-32-x-32-pixel-9-hz-built-in-digital-camera-2362843>, 2023.
- [44] H.H. Istepanian, Towards sustainable energy efficiency in Iraq. <https://www.bayancenter.org/en/wp-content/uploads/2020/08/16449.pdf>, 2020.
- [45] A.W. Abbood, K.M. Al-Obaidi, H. Awang, A.M. Abdul Rahman, Achieving energy efficiency through industrialized building system for residential buildings in Iraq. *Int. J. Sustain. Built Environ.* 4 (2015) 78–90, <https://doi.org/10.1016/j.ijsbe.2015.02.002>.
- [46] Ministry of Agriculture, Iraqi Agrometeorological network, (n.d.). <http://www.agromet.gov.iq/>.
- [47] P.M. Toure, Y. Dieye, P.M. Gueye, V. Sambou, S. Bodian, S. Tiguampo, Experimental determination of time lag and decrement factor, *Case Stud. Constr. Mater.* 11 (2019), e00298, <https://doi.org/10.1016/j.cscm.2019.e00298>.
- [48] P.K.S. Rathore, S.K. Shukla, An experimental evaluation of thermal behavior of the building envelope using macroencapsulated PCM for energy savings, *Renew. Energy* 149 (2020) 1300–1313, <https://doi.org/10.1016/j.renene.2019.10.130>.
- [49] N. Beemkumar, D. Yuvarajan, M. Arulprakasajothi, K. Elangovan, T. Arunkumar, Control of room temperature fluctuations in the building by incorporating PCM in the roof, *J. Therm. Anal. Calorim.* 30 (2020), 101536, <https://doi.org/10.1007/s10973-019-09226-0>.
- [50] M. Sovetova, S.A. Memon, J. Kim, Energy savings of PCM-incorporated building in hot dry climate, *Key Eng. Mater.* 821 KEM (2019) 518–524, <https://doi.org/10.4028/www.scientific.net/KEM.821.518>.
- [51] S. Ramakrishnan, J. Sanjayan, X. Wang, Experimental research on using form-stable PCM-integrated cementitious composite for reducing overheating in buildings, *Buildings*. 9 (2019) 57, <https://doi.org/10.3390/buildings9030057>.
- [52] S. Wi, S. Yang, J.H. Park, S.J. Chang, S. Kim, Climatic cycling assessment of red clay/perlite and vermiculite composite PCM for improving thermal inertia in buildings, *Build. Environ.* 167 (2020), 106464, <https://doi.org/10.1016/j.buildenv.2019.106464>.
- [53] J.C. Lam, C.L. Tsang, D.H.W. Li, S.O. Cheung, Residential building envelope heat gain and cooling energy requirements, *Energy* 30 (2005) 933–951, <https://doi.org/10.1016/j.energy.2004.07.001>.
- [54] ANSI/ASHRAE Standard 55-2010, Thermal environmental conditions for human occupancy, *Encycl. Financ.* (2010), [https://doi.org/10.1007/0-387-26336-5\\_1680](https://doi.org/10.1007/0-387-26336-5_1680).
- [55] A. Sharma, N. Sengar, Heat gain study of a residential building in hot-dry climatic zone on basis of three cooling load methods, *Eur. J. Eng. Res. Sci.* 4 (2019) 186–194, <https://doi.org/10.24018/ejers.2019.4.9.1508>.
- [56] Z.X. Li, A.A.A.A. Al-Rashed, M. Rostamzadeh, R. Kalbasi, A. Shahsavari, M. Afrand, Heat transfer reduction in buildings by embedding phase change material in multi-layer walls: effects of repositioning, thermophysical properties and thickness of PCM, *Energy Convers. Manag.* 195 (2019) 43–56, <https://doi.org/10.1016/j.enconman.2019.04.075>.
- [57] H.-F. Ashrae, Chapter 22, *Thermal and Moisture Control in Insulated Assemblies—Fundamentals*, Am. Soc. Heating, Refrig. Air-Conditioning Eng. Inc., Atlanta, 1997.
- [58] J. Lei, J. Yang, E.-H. Yang, Energy performance of building envelopes integrated with phase change materials for cooling load reduction in tropical Singapore, *Appl. Energy* 162 (2016) 207–217, <https://doi.org/10.1016/j.apenergy.2015.10.031>.
- [59] A.C. Rai, Energy performance of phase change materials integrated into brick masonry walls for cooling load management in residential buildings, *Build. Environ.* 199 (2021), 107930, <https://doi.org/10.1016/j.buildenv.2021.107930>.
- [60] R.A. Kishore, M.V.A.A. Bianchi, C. Booten, J. Vidal, R. Jackson, Optimizing PCM-integrated walls for potential energy savings in US buildings, *Energy Build.* 226 (2020), 110355, <https://doi.org/10.1016/j.enbuild.2020.110355>.
- [61] A. Amirahmad, A.M. Maglad, J. Mustafa, G. Cheraghian, Loading PCM into buildings envelope to decrease heat gain-performing transient thermal analysis on nanofluid filled solar system, *Front. Energy Res.* 9 (2021), 727011, <https://doi.org/10.3389/fenrg.2021.727011>.
- [62] H.J. Alqallaf, E.M. Alawadhi, Concrete roof with cylindrical holes containing PCM to reduce the heat gain, *Energy Build.* 61 (2013) 73–80, <https://doi.org/10.1016/j.enbuild.2013.01.041>.
- [63] M. Hamdani, S.M.E.A. Bekkouch, S. Al-Saadi, M.K. Cherier, R. Djeflal, M. Zaiani, Judicious method of integrating phase change materials into a building envelope under Saharan climate, *Int. J. Energy Res.* 45 (2021) 18048–18065, <https://doi.org/10.1002/er.6951>.
- [64] C.G. Rangel, C.I. Rivera-Solorio, M. Gijón-Rivera, S. Mousavi, The effect on thermal comfort and heat transfer in naturally ventilated roofs with PCM in a semi-arid climate: an experimental research, *Energy Build.* 274 (2022), 112453, <https://doi.org/10.1016/j.enbuild.2022.112453>.
- [65] P. Saikia, M. Pancholi, D. Sood, D. Rakshit, Dynamic optimization of multi-retrofit building envelope for enhanced energy performance with a case study in hot Indian climate, *Energy* 197 (2020), 117263, <https://doi.org/10.1016/j.energy.2020.117263>.
- [66] V. Sharma, A.C. Rai, Performance assessment of residential building envelopes enhanced with phase change materials, *Energy Build.* 208 (2020), 109664, <https://doi.org/10.1016/j.enbuild.2019.109664>.
- [67] N. Elawady, M. Bekheit, A.A. Sultan, A. Radwan, Energy assessment of a roof-integrated phase change materials, long-term numerical analysis with experimental validation, *Appl. Therm. Eng.* 202 (2022), 117773, <https://doi.org/10.1016/j.applthermaleng.2021.117773>.
- [68] M.R. Elmarghany, A. Radwan, M.A. Shouman, A.A. Khater, M.S. Salem, O. Abdelrehim, Year-long energy analysis of building brick filled with phase change materials, *J. Energy Storage* 50 (2022), 104605, <https://doi.org/10.1016/j.est.2022.104605>.
- [69] C. Cárdenas-Ramírez, M.A. Gómez, F. Jaramillo, A.F. Cardona, A.G. Fernández, L. F. Cabeza, Experimental steady-state and transient thermal performance of materials for thermal energy storage in building applications: from powder SS-PCMs to SS-PCM-based acrylic plaster, *Energy*. 250 (2022), 123768, <https://doi.org/10.1016/j.energy.2022.123768>.
- [70] P. Sangwan, H. Mehdizadeh-Rad, A.W.M. Ng, M.A.U.R. Tariq, R.C. Nnachi, Performance evaluation of phase change materials to reduce the cooling load of buildings in a tropical climate, *Sustain.* 14 (2022) 3171, <https://doi.org/10.3390/su14063171>.
- [72] S. Kumar, S. Arun Prakash, V. Pandiyarajan, N.B. Geetha, V. Antony Aroul Raj, R. Velraj, Effect of phase change material integration in clay hollow brick composite in building envelope for thermal management of energy efficient buildings, *J. Build. Phys.* 43 (2019) 351–364, <https://doi.org/10.1177/1744259119867462>.